

# Pulsar braking and the $P - \dot{P}$ diagram

Simon Johnston<sup>1,2\*</sup> and A. Karastergiou<sup>3,4,5</sup>

<sup>1</sup>CSIRO Astronomy and Space Science, Australia Telescope National Facility, PO Box 76, Epping, NSW 1710, Australia

<sup>2</sup>Max-Planck-Institut für Radioastronomie (MPIfR), Auf dem Hügel 69, D-53121 Bonn, Germany

<sup>3</sup>Oxford Astrophysics, Denys Wilkinson Building, Keble Road, Oxford, OX1 3RH, UK.

<sup>4</sup>Physics Department, University of the Western Cape, Cape Town 7535, South Africa

<sup>5</sup>Department of Physics and Electronics, Rhodes University, PO Box 94, Grahamstown 6140, South Africa

Accepted 14 February 2017. Received 14 February 2017; in original form 14 February 2017

## ABSTRACT

The location of radio pulsars in the period-period derivative ( $P - \dot{P}$ ) plane has been a key diagnostic tool since the early days of pulsar astronomy. Of particular importance is how pulsars evolve through the  $P - \dot{P}$  diagram with time. Here we show that the decay of the inclination angle ( $\alpha$ ) between the magnetic and rotation axes plays a critical role. In particular,  $\dot{\alpha}$  strongly impacts on the braking torque, an effect which has been largely ignored in previous work. We carry out simulations which include a negative  $\dot{\alpha}$  term, and show that it is possible to reproduce the observational  $P - \dot{P}$  diagram without the need for either pulsars with long birth periods or magnetic field decay. Our best model indicates a birth rate of 1 radio pulsar per century and a total Galactic population of  $\sim 20000$  pulsars beaming towards Earth.

**Key words:** pulsars

## 1 INTRODUCTION

Upon the discovery of a radio pulsar, its position in the sky, its spin period,  $P$ , and dispersion measure are immediately known. The technique of pulsar timing subsequently allows the slow-down rate,  $\dot{P}$ , to be determined. From the very early days of pulsar astronomy, therefore, pulsars could be placed on the  $P - \dot{P}$  plane. Figure 1 shows the modern  $P - \dot{P}$  diagram for 1600 of the known pulsars. In this figure we have excluded all re-cycled pulsars to concentrate on the bulk of the slow pulsar population.

If we assume that the pulsar is a magnetic dipole rotating in a vacuum, the surface magnetic field strength,  $B$ , is given by

$$B = \sqrt{\frac{3c^3 I}{8\pi^2 R^6 \sin^2 \alpha}} P \dot{P} \quad (1)$$

where  $c$  is the speed of light,  $I$  is the moment of inertia of the star,  $R$  is its radius and  $\alpha$  is the inclination angle between the rotation and magnetic axes. If therefore one assumes that  $I$  and  $R$  are the same for all pulsars and  $\sin^2 \alpha = 1$ , one can draw lines of constant  $B$  onto the  $P - \dot{P}$  diagram (see Figure 1). Similarly, the spin-down energy,  $\dot{E}$ , can be written

$$\dot{E} = 4\pi^2 I \frac{\dot{P}}{P^3} \quad (2)$$

and again this allows for lines of constant  $\dot{E}$  on the  $P - \dot{P}$  diagram. Finally, the characteristic age,  $\tau_c$  of the pulsar is computed via

$$\tau_c = \frac{P}{2\dot{P}} \quad (3)$$

The value of  $\tau_c$  is equal to the true age under the assumption that the initial spin period of the pulsar is much less than its current period and that dipolar magnetic braking is the sole cause of the spin-down. Lines of constant  $\tau_c$  are also included in Figure 1.

Under the assumptions made above, the  $P - \dot{P}$  diagram can be used as an evolutionary tool. Young pulsars live at the top left of the diagram with small  $P$  and high  $\dot{P}$ . The magnetars, with their high  $B$ -fields live in the top right of the diagram. The bulk of the pulsars form a roughly circular shape in the diagram. Very few pulsars have  $\dot{E}$  below  $10^{30}$  ergs  $s^{-1}$ ; this marks the so-called death-line below which it is believed radio emission ceases to be viable.

More generally, the spin-down of a pulsar can be written in the form

$$\dot{\nu} = -K\nu^n \quad (4)$$

where here  $\nu$  and  $\dot{\nu}$  are the spin frequency and its derivative,  $K$  is constant and  $n$  is the braking index. Taking the time derivative of Equation 4 yields

$$n = \frac{\nu \ddot{\nu}}{\dot{\nu}^2} \quad (5)$$

and so  $n$  can in principle be measured if  $\ddot{\nu}$  can be obtained. If

\* email: Simon.Johnston@csiro.au

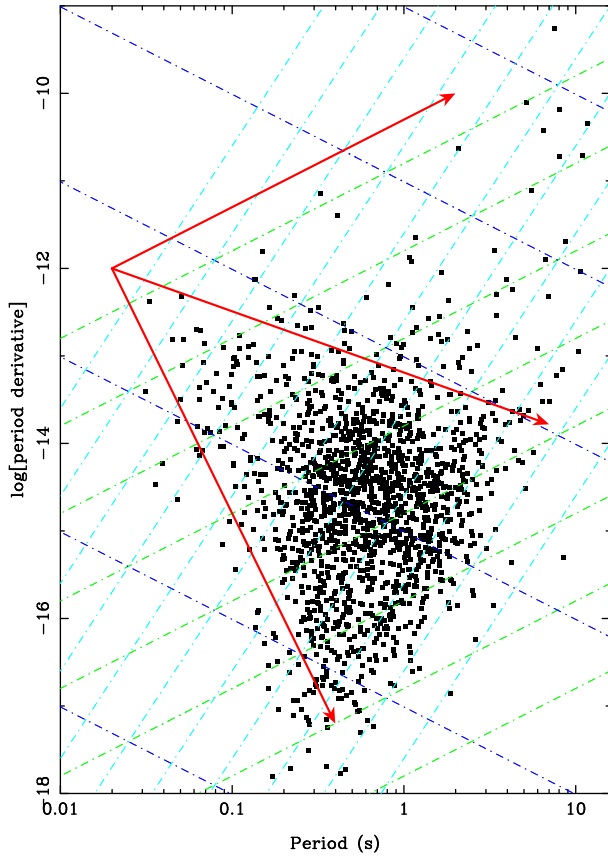


**Figure 1.** The  $P - \dot{P}$  diagram for 1600 known pulsars. Lines of constant  $B$  are in blue, line of constant  $n$  are green and line of constant  $\dot{B}$  are light blue. From an initial position at  $P = 20$  ms,  $\dot{P} = 10^{-12}$ , the red arrows show time-evolution through the diagram for  $n = 1.0, 2.7$  and  $6.0$  from top to bottom.

both  $K$  and  $n$  are constant in time, a pulsar will then follow a track in the  $P - \dot{P}$  diagram with a slope of  $2 - n$ . Theoretical expectations are that if the torque is dominated by an outflowing wind then  $n = 1$ , if magnetic dipole dominated then  $n = 3$ , and if magnetic quadrupole dominated then  $n = 5$  in the absence of other effects (Alvarez & Carramiñana 2004). Hamil et al. (2015) have shown that  $n$  can deviate from these values because of the changing  $I$  as the star spins down.

Two important modifications to this simple picture, magnetic field decay and alignment of the spin and magnetic axes, were outlined in Tauris & Konar (2001). They showed that, in this case, the braking index is a function of time and depends on the time-evolution of  $B$  and  $\alpha$  in the following way:

$$n(t) = 3.0 - \frac{3c^3 I \dot{B}(t)}{R^6 B^3(t) \sin^2 \alpha(t) \Omega^2(t)} - \frac{3c^3 I \cos \alpha(t) \dot{\alpha}(t)}{R^6 B^2(t) \sin^3 \alpha(t) \Omega^2(t)} \quad (6)$$

In this equation, the second term contains the time derivative of the magnetic field,  $\dot{B}$ , with the third term relating to the time derivative of the inclination axis,  $\dot{\alpha}$ .

Unfortunately  $\ddot{\nu}$  is small and difficult to measure, making  $n$  hard to determine with any accuracy in all but a handful of young pulsars. Measured values of  $n$  range

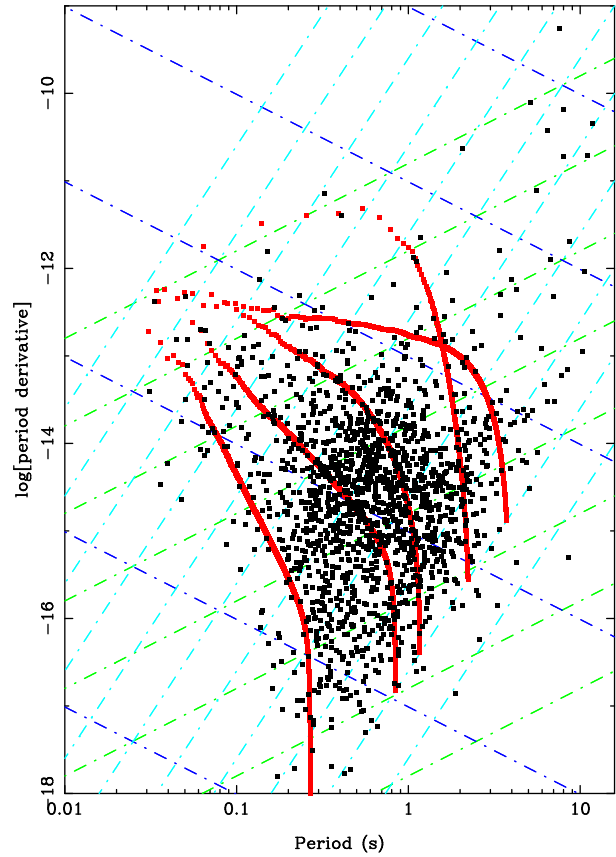


**Figure 2.** As for Figure 1. From an initial position at  $P = 20$  ms,  $\dot{P} = 10^{-12}$ , the red lines denote time-evolution through the diagram in steps of 1000 yr according to Equation 6 for different initial values of  $n$ . Evolutionary tracks end once the pulsar has crossed the death line.

from 0.9 in PSR J1734–3333 (Espinoza et al. 2011) to 3.15 for PSR J1640–4631 (Archibald et al. 2016) though Marshall et al. (2016) have recently reported  $n$  close to zero for PSR B0540–69 in the Large Magellanic Cloud. Astonishingly, the braking index of PSR J1846–0258 changed from 2.65 to 2.19 in less than a decade (Archibald et al. 2015) and a smaller change was seen in PSR J1119–6127 (Antonopoulou et al. 2015). This implies that substantial torque changes can be applied to the star on short timescales. We also note that Johnston & Galloway (1999) proposed a way to obtain  $n$  without the need to measure  $\ddot{\nu}$  in a fully coherent solution. In their paper, they reported a number of pulsars with high values of  $|n|$  (and small error bars) over the timescale of a decade. They surmised that these high values were caused by recovery from (unseen) glitches but whatever the cause, high values of  $n$  are clearly plausible.

In addition to direct measurements of  $n$ , there is a mounting body of evidence for torque changes on short timescales in many, if not all, pulsars. The class of pulsars known as ‘intermittents’ show that  $\dot{P}$  changes significantly between the ‘on’ and ‘off’ states likely due to the presence of plasma in the magnetosphere (Kramer et al. 2006). Lyne et al. (2010) showed state (profile) changes accompanied by  $\dot{P}$  changes in a large number of pulsars, a study backed up by Brook et al. (2016). Torque changes

may also be induced through interaction with asteroids (Shannon et al. 2013; Brook et al. 2014) or free precession (Kerr et al. 2016). With these results in mind, we therefore modify Equation 6 to read

$$n(t) = n_0 - \frac{3c^3 I \dot{B}(t)}{R^6 B^3(t) \sin^2 \alpha(t) \Omega^2(t)} - \frac{3c^3 I \cos \alpha(t) \dot{\alpha}(t)}{R^6 B^2(t) \sin^3 \alpha(t) \Omega^2(t)} + \text{TN}(t) \quad (7)$$

where now  $n_0$  is the initial braking index and  $\text{TN}(t)$  is a random component of the braking index due to effects of state changes, timing noise and/or intermittency. This will be discussed further in Section 3.

A major unresolved challenge in pulsar astronomy is determining where pulsars are born in the  $P - \dot{P}$  diagram and how then they evolve through the diagram with time. We explore this issue further in Section 2. In Section 3 we outline our simulation, present the results in Section 4, discuss the implications in Section 5 before concluding in Section 6.

## 2 EVOLUTION IN THE $P - \dot{P}$ DIAGRAM

Two major problems confront us when we study the  $P - \dot{P}$  diagram. The first is that young pulsars such as the Crab pulsar ( $P \simeq 33$  ms,  $\dot{P} \simeq 4 \times 10^{-13}$ ) appear to have magnetic fields larger than older pulsars. Hence, one idea is that the magnetic field decays as pulsars get older as was first postulated by Gunn & Ostriker (1970). This remains controversial as more modern studies still press the case for (e.g. Gonthier et al. 2004) and against (e.g. Lorimer et al. 1997) field decay. Theoretical work in this area also has not reached a consensus, suggesting field decay is either unimportant (Goldreich & Reisenegger 1992) or relatively rapid (Gullón et al. 2014; Igoshev & Popov 2015) over the pulsar lifetime. We note that field decay almost certainly occurs during episodes of mass accretion but this is not relevant to the general population of isolated pulsars under consideration here. The second issue is whether all pulsars are born like the Crab pulsar with a fast ( $\simeq 20$  ms) initial spin period and high magnetic field, or whether the  $P - \dot{P}$  diagram can only be explained by postulating an ‘injection’ of pulsars with much slower ( $\sim 500$  ms) birth periods. This idea, first championed by Vivekanand & Narayan (1981), still has recent proponents (e.g. Vranesovic et al. 2004) but other studies find no need for long period at birth (e.g. Gonthier et al. 2002).

Population studies which attempt to replicate the properties of the observed pulsars follow two different approaches. The first is to take a snapshot of the Galaxy as it appears today and match it to the observed population (see e.g. Bates et al. 2014). The second is an *ab initio* approach which has evolution of pulsars from birth onwards. As a fine example of the latter genre, we consider the comprehensive study of the birth and evolution of isolated radio pulsars by Faucher-Giguère & Kaspi (2006). The major conclusions of their paper are that (i) magnetic field decay is not significant, (ii) the luminosity  $L$  of a pulsar is proportional to  $\sqrt{\dot{E}}$ , (iii) the initial spin period has a mean of 300 ms with a wide distribution. One of the assumptions in Faucher-Giguère & Kaspi (2006) is that the braking index

of a pulsar has a constant value over the pulsar’s lifetime and although they explored a distribution in this constant they did not attempt to model evolution of  $n$  as a function of time. Similarly, more recent work by Ridley & Lorimer (2010) investigated random values for  $n$  at birth but did not consider  $n$  to vary with time. Both groups include  $\alpha$  decay in their simulations, and yet failed to include time-variable  $n$  even though this is implied via Equation 7.

A more theoretical approach was taken by Gullón et al. (2014) and they take proper account of the time evolution of the magnetic field and the inclination angle. In addition, they include the effects of plasma in the magnetosphere and further consider the magneto-thermal evolution of the star. They strongly favour a model where  $\dot{B} < 0$  and a power-law decay of  $\alpha$ .

### 2.1 Evidence for non-zero $\dot{\alpha}$

Only one direct observational measurement of  $\dot{\alpha}$  has been made in a normal, isolated pulsar. Lyne et al. (2013) reported on 22 years of timing of the Crab pulsar which shows that  $\alpha$  is increasing at a rate of 0.62 degrees per century. Statistically, however, it appears the opposite is the case. Tauris & Manchester (1998) examined the distribution of  $\alpha$  in the known pulsar population under the assumption of filled circular beams and measurements of the pulse width. They showed that there were many more small values of  $\alpha$  than expected and concluded that alignment must occur (i.e. that  $\dot{\alpha} < 0$ ) on a timescale of  $10^7$  yr. Weltevrede & Johnston (2008) came to very similar conclusions by attacking the problem in a different way. They showed that the fraction of pulsars with interpulses was inconsistent with a random distribution of  $\alpha$ . They concluded that although  $\alpha$  was random at birth,  $\dot{\alpha}$  must be less than zero so that the magnetic and rotational axes align with time. Jones (1976) argues that alignment only begins to occur when the pulsar age exceeds  $10^4$  yr, once the temperature-dependent dissipative torque becomes negligible. If this is correct, the expectation is that the value of  $\dot{\alpha}$  in the Crab will change sign in the future. The form of  $\alpha$  decay has been considered theoretically by Philippov et al. (2014) for pulsars with and without plasma loading of the magnetosphere. For the vacuum case, pulsars align (unrealistically) fast. With plasma loading the alignment time is much longer and the form of the decay is power-law rather than exponential. Even in this case, however, the timescale is shorter than observers are comfortable with. In light of the uncertainties in the theoretical models, we assume an exponential decay of  $\alpha$  with a timescale of order  $10^7$  yr.

We note that in the case of the very old millisecond pulsars and the neutron stars in X-ray binary systems, that  $\alpha \neq 0$ . However, these pulsars have had episodes of mass accretion from their companion star. Mass accretion is expected to cause magnetic field decay in these systems (as first postulated by Alpar et al. 1982) and almost certainly causes a re-arrangement of the magnetic field structure and hence  $\alpha$  (Payne & Melatos 2004).

### 3 SIMULATIONS

The thinking behind the introduction of a variable braking index is as follows: if all pulsars are born with parameters similar to that of the Crab pulsar, can we use braking index alone to replicate the  $P - \dot{P}$  diagram without the need for either magnetic field decay or for pulsars born spinning slowly? We have seen that since the publication of [Faucher-Giguère & Kaspi \(2006\)](#), our knowledge of the braking indices of pulsars has changed dramatically. It now appears evident that not only is there a wide range of  $n$  but that  $n$  can change significantly even on short timescales. Furthermore, as listed above, the evidence for  $\alpha$ -decay is strong and this implies a long-term evolution of  $n$  as shown by [Tauris & Konar \(2001\)](#).

First consider straight line tracks in the  $P - \dot{P}$  diagram (recalling that for a constant  $n$ , the evolution in the diagram follows a slope of  $2-n$ ) for a pulsar with initial parameters of  $P = 20$  ms,  $\dot{P} = 10^{-12}$ . In order for this pulsar to reach the bottom left of the bulk of the population,  $n$  must be 6.0. For it to reach the bottom right of the population,  $n$  must be 2.7 while to reach the magnetars at the extreme top right then  $n$  must be 1.0. Figure 1 shows these tracks. Now consider that  $n$  can vary with time as in Equation 6. Figure 2 shows five example tracks with  $\dot{B} = 0$  and an exponential decay of  $\alpha$  on a timescale of  $10^7$  yr.

Several ideas then manifest themselves. The first is that  $n$  is fixed at birth, but takes a wide range of values sufficient to be able to populate the  $P - \dot{P}$  plane. This idea was tested by [Faucher-Giguère & Kaspi \(2006\)](#) and [Ridley & Lorimer \(2010\)](#) and found not to provide a good match to the observed population. The second is that  $n$  be time dependent and perform a random walk over the allowed parameter space. A simple simulation therefore involves using Equation 7 with  $\dot{B} = \dot{\alpha} = 0$ , picking an initial value for  $n_0$  and then allowing  $TN(t)$  to provide short timescale variations. Finally,  $n$  varies according to Equation 7 and different combinations of  $\dot{B}$  and  $\dot{\alpha}$  can be trialled in addition to the random component  $TN(t)$ .

In our simulation, we build on the work of others by fixing many of the initial parameters. For the spatial distribution of pulsars we assume the form of the radial distribution given by [Lorimer \(2004\)](#)

$$\rho_r(R) = K_r R^i e^{-R/\sigma_r} \quad (8)$$

where  $\rho_r(R)$  is the density of pulsars (per kpc<sup>2</sup>) at radius  $R$  (in kpc) from the Galactic Centre and  $K_r$ ,  $i$  and  $\sigma_r$  are constants with values of 64.6 kpc<sup>-2</sup>, 2.35 and 1.258 kpc respectively. For the  $z$ -height distribution we use an exponential with a scale height of 330 pc ([Lorimer et al. 2006](#)). For any given pulsar, therefore, we pick a random distance from Earth,  $d$ , based on these distributions. We assume that  $\alpha$  is randomly distributed at birth (i.e. that the probability distribution is  $\sin(\alpha)$ , see also [Gullón et al. 2014](#)) but exponentially decays towards  $\alpha = 0$  with a time constant of  $5 \times 10^7$  y ([Tauris & Manchester 1998](#); [Weltevrede & Johnston 2008](#)). This is a crucial feature of our model because the beaming fraction of pulsars with low  $\alpha$  is smaller than at high  $\alpha$  and we have seen from Equation 7 how  $\dot{\alpha}$  affects the value of  $n$ . We take the half-opening angle  $\rho$  of a pulsar's radio beam (in degrees) at a canonical observing frequency of 1.4 GHz

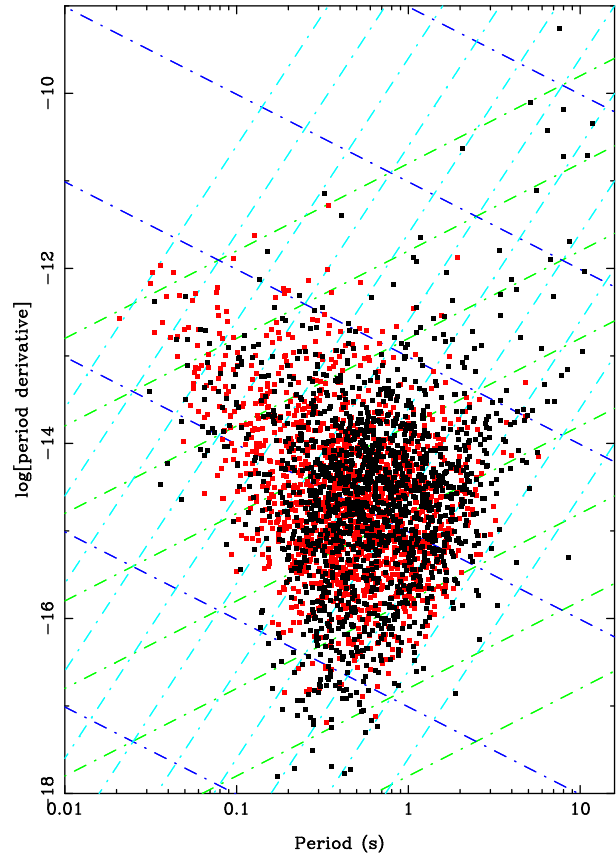


**Figure 3.**  $P - \dot{P}$  diagram for the known pulsars (black points) and the pulsars detected in the simulation (red points).

to be

$$\rho = 6.8P^{-0.5}. \quad (9)$$

This is slightly larger than generally assumed ([Kramer et al. 1994](#)) but in line with the results of [Mitra & Rankin \(2002\)](#). The combination of  $\alpha$  and  $\rho$  yields a beaming fraction, the probability that the pulsar is beaming towards Earth (see e.g. [Tauris & Manchester 1998](#)). If the pulsar is beaming towards Earth we then pick a value of the impact parameter,  $\beta$  between  $-\rho$  and  $+\rho$ . The combination of  $\rho$ ,  $\alpha$  and  $\beta$  then yields the observed pulse width,  $w$  (e.g. [Gil et al. 1984](#)). We also introduce a death line at  $\dot{E} = 10^{30}$  ergs<sup>-1</sup> as do [Faucher-Giguère & Kaspi \(2006\)](#).

We want to test the idea that all pulsars are born like the Crab, so we fix the birth parameters at  $P = 20$  ms,  $\dot{P} = 10^{-12}$ . Pulsar ages are evenly distributed in steps of the birth rate,  $B_R$ , up to some maximum age,  $T_{\max}$  so that the number of pulsars is  $T_{\max}/B_R$ . In principle  $T_{\max}$  could be set to the age of the Galaxy; in practice we find that  $10^8$  y is sufficient as pulsars older than this are either too faint to be detectable or fall below the death line. The value of  $B_R$  ranges from 3 per century to less than 1 per century with the arguments summarised in [Keane & Kramer \(2008\)](#). We return to the value of this parameter in the next section.

This leaves us requiring a luminosity law, in order to determine whether or not a pulsar beaming towards Earth is actually detectable giving the sensitivity of radio telescopes. Discussion over the form of the luminosity distribution of radio pulsars has continued in the literature for more than 30



years, and is well summarised in [Faucher-Giguère & Kaspi \(2006\)](#). An accepted form for the luminosity law is

$$\log L = \log(L_0 P^{\epsilon_1} \dot{P}^{\epsilon_2}) + L_c. \quad (10)$$

In the recent literature, [Faucher-Giguère & Kaspi \(2006\)](#) and [Gullón et al. \(2014\)](#) have  $\epsilon_1 = -1.5$ ,  $\epsilon_2 = 0.5$  whereas [Ridley & Lorimer \(2010\)](#) have  $\epsilon_1 = -1.0$ ,  $\epsilon_2 = 0.5$  and [Bates et al. \(2014\)](#) have  $\epsilon_1 = -1.4$ ,  $\epsilon_2 = 0.5$ . Once the luminosity is known we can convert to a (pseudo-) flux density;  $S = Ld^{-2}$ .

It is beyond the scope of this paper to reproduce the complex selection effects of real pulsar surveys. Rather, we make the conversion from luminosity to signal-to-noise ratio (SNR) via

$$\text{SNR} = \frac{L}{d^2 S_0} \sqrt{\frac{P - w}{w}} \quad (11)$$

using a simple scaling term  $S_0$  which is adequate for our purposes. The term inside the square root comes from the fact that pulsars are not found via continuum imaging, but rather through a Fourier technique which has the consequence that narrow pulses are easier to detect than broad pulses of the same power ([Dewey et al. 1985](#)).

The simulation therefore proceeds as follows. Initial parameters  $P$ ,  $\dot{P}$ ,  $d$  and  $\alpha$  are chosen. The initial braking index,  $n_0$  is drawn from a normal distribution with a mean of 2.8 and a  $\sigma$  of 1.0. The pulsar evolves in time, and values of  $P$ ,  $\dot{P}$ ,  $\alpha$  and  $n$  (according to Equation 7) are updated. The form of  $\text{TN}(t)$  is such that every 1000 y, a random value is picked from a Gaussian distribution with a mean of the current value of  $n$  and a  $\sigma$  of  $n/3$ . Once the pulsar has reached the appropriate age,  $\rho$ ,  $\beta$ ,  $\dot{E}$ ,  $L$  and SNR are computed. A pulsar is deemed detectable if (a) it is beaming towards Earth, (b) it has  $\text{SNR} > 10$  (according to Equation 11 above) and (c) its  $\dot{E}$  places it above the death line. The ensemble of detected pulsars can then be compared with the known pulsar population.

## 4 RESULTS OF THE SIMULATION

### 4.1 Luminosity law and birth rate

As with all population studies, the parameters of the luminosity law (Equation 10) are critical to the output of the simulation. We set  $L_c = 0$ . Clearly, in the observed population there can be large differences in luminosity for pulsars with similar  $P$  and  $\dot{P}$ . In a statistical sense however,  $L_c$  makes little difference to the outcome of the simulations.

We initially tested  $\epsilon_1 = \epsilon_2 = 0.0$  so that the luminosity is independent of  $P$  and  $\dot{P}$ . This yielded a large number of detected pulsars with long periods and a ‘pile-up’ of detections close to the death line. This is clearly in disagreement with the observations, a conclusion also reached by others ([Faucher-Giguère & Kaspi 2006](#); [Ridley & Lorimer 2010](#)).

We then tested  $\epsilon_1 = -1.5$ ,  $\epsilon_2 = 0.5$ , the values favoured by [Faucher-Giguère & Kaspi \(2006\)](#). This is appealing because it implies that  $L \propto \dot{E}^{1/2}$  similar to that seen in  $\gamma$ -ray pulsars ([Perera et al. 2013](#)). We find that this luminosity law results in the detection of too many young, short period pulsars compared to the observed distribution. This is because  $\dot{E}$  decreases by 8 orders of magnitude over the lifetime of a pulsar and so the luminosity law is strongly biased

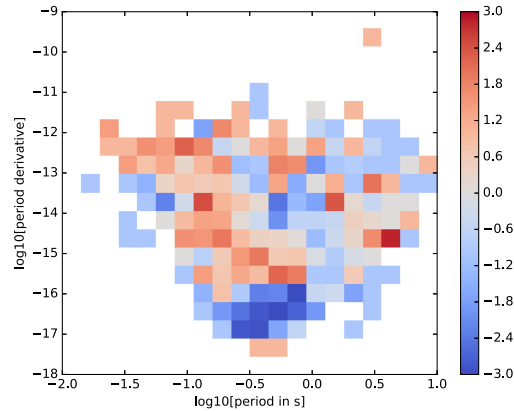


**Figure 4.** The difference between the observed and simulated  $P - \dot{P}$  diagram, colour coded using Eq. 12. Red signifies an over-abundance of simulated pulsars, blue an under-abundance.

towards high  $\dot{E}$  pulsars. To counteract this problem, the general solution is to postulate long periods at birth as both [Faucher-Giguère & Kaspi \(2006\)](#) and [Bates et al. \(2014\)](#) do.

Clearly though if  $\epsilon_1 = \epsilon_2 = 0.0$  produces too many old pulsars and  $\epsilon_1 = -1.5$ ,  $\epsilon_2 = 0.5$  produces too many young pulsars, an alternative solution would be to have a luminosity law somewhere in between these two possibilities. Indeed, we find an acceptable fit to the observed pulsars can be made by setting  $\epsilon_1 = -0.75$ ,  $\epsilon_2 = 0.25$ .

We find the best fit to the data is obtained with  $B_R$  set to 1 per century. Higher values of  $B_R$  result in the detection of too many short period pulsars compared to the observed population. Our value is significantly lower than the 2.8 per century found by [Faucher-Giguère & Kaspi \(2006\)](#) and the  $\sim 3$  per century in [Gullón et al. \(2014\)](#) but within the errors of the [Lorimer et al. \(2006\)](#) and [Vranesevic et al. \(2004\)](#) values.

### 4.2 Model performance

Figure 3 shows the comparison between the simulation and the known pulsar population. As [Faucher-Giguère & Kaspi \(2006\)](#) discussed, it is difficult to quantitatively assess the goodness-of-fit for these type of simulations. The Kolmogorov-Smirnov (K-S) test is rather a blunt instrument and does not work well for multi-dimensional data. Although the K-S test could be used on individual parameters such as  $P$  and  $\dot{P}$ , these parameters are not independent making it hard to judge the output from the K-S test. We therefore proceeded as follows: We generate 2D histograms in the  $P - \dot{P}$  plane for both the observed and simulated populations. The histograms are generated using a set of 20 bins of equal width in logarithm space along each direction, and counting the number of simulated pulsars ( $N_{\text{sim}}$ ) and the number of observed pulsars ( $N_{\text{obs}}$ ) for each 2D bin. We then define the significance of the difference in the pairs of numbers,  $R$ , through

$$R = \frac{N_{\text{sim}} - N_{\text{obs}}}{\sqrt{N_{\text{sim}} + N_{\text{obs}}}} \quad (12)$$

and assign a colour scale to the range of values of  $R$ .

Figure 4 shows a visual representation of equation 12 and although the figure cannot be used in a statistical sense, it is indicative of the goodness-of-fit of the model. The model performs most poorly towards the bottom left of the  $P - \dot{P}$  diagram, where the simulation underpredicts the observed numbers. Lorimer et al. (2004) speculate that this part of the diagram contains pulsars originally part of a binary system. Their magnetic field then decays and their spin period decreases as a result of accretion of material from the binary companion before the system disrupts after the second supernova (Belczynski et al. 2010). This provides a plausible explanation for the surfeit of pulsars in this part of the diagram. Our model also somewhat underestimates the magnetar population, those pulsars with long periods and high  $\dot{P}$ . Although some evolutionary tracks head in the right direction (see Figure 2),  $\alpha$  decay pulls them downwards before they reach the magnetar area of the  $P - \dot{P}$  diagram. It remains unclear whether magnetars are a separate class of pulsars or whether indeed they arise from evolution from a different part of  $P - \dot{P}$  space (Keane & Kramer 2008; Espinoza et al. 2011). Furthermore, magnetars appear to have wide beams and do not conform to Equation 9. This presumably implies that their beaming fraction is much larger than our simulation supposed, causing our model to underestimate their population.

## 5 DISCUSSION

### 5.1 Differences with other studies

There is strong evidence that  $\alpha$  decays with time (Tauris & Manchester 1998; Weltevrede & Johnston 2008; Philippov et al. 2014) and therefore that  $n$  is time-variable according to Equation 7. This is an integral part of our model. Ridley & Lorimer (2010) consider  $\alpha$  decay in detail but they do not make the important connection between this and the braking index. Their pulsars therefore do not move correctly in  $P - \dot{P}$  space.

The optimum model of Faucher-Giguère & Kaspi (2006) does not include  $\alpha$  decay and assumes a constant braking index of 3. Pulsars are therefore forced to move along lines of constant  $B$  (see Figure 1). The observed pulsars have a wide range of  $B$  and so their model must reflect this in the birth parameters. Indeed their model has  $\sigma = 0.55$  (in the log) for the birth  $B$  field. In addition, their luminosity law forces pulsars to be born with relatively long initial spin periods to prevent an overabundance of short period pulsars. In our model, pulsars have high  $B$  and short  $P$  at birth. Although  $B$  does not decay, the *apparent*  $B$  (as computed via Equation 1) drops because  $n$  becomes larger than 3 as the pulsar ages. At the same time, we have flattened the dependence of  $L$  on  $P$ , which alleviates the young pulsar problem. It does not create an old pulsar problem, because old pulsars have smaller  $\alpha$  which reduces their beaming fraction and increases the pulse width which reduces their detectability.

The work of Gonthier et al. (2004) includes the effect of  $B$ -field decay with their optimal model having a decay timescale of only 2.8 Myr. Initial spin periods are short, and initial values of  $B$  are generally higher than found by other groups. They also include a full description of core-cone radio beams which modifies their luminosity law which

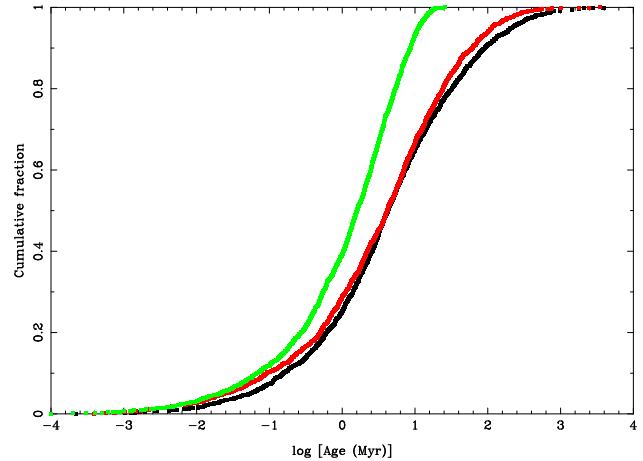


**Figure 5.** Cumulative distribution of the characteristic ages of the known population (black) and the simulated detections (red) with the true ages of the simulated pulsars shown in green.

has  $\epsilon_1 = -1.3$ ,  $\epsilon_2 = 0.5$ . They do not consider  $\alpha$  decay. In some ways, our results reflect theirs; they set  $\dot{\alpha} = 0$  and have  $\dot{B} < 0$  whereas we have  $\dot{\alpha} < 0$  and  $\dot{B} = 0$  which has the same effect on  $n$  according to Equation 7. However, as explained above smaller values of  $\alpha$  for older pulsars reduces their detectability which we believe is a crucial difference in the modelling.

Finally Gullón et al. (2014) include both  $B$ -field and  $\alpha$  decay in their models. Although their results are rather agnostic as to  $B$ -field decay they strongly prefer a power-law decay of  $\alpha$ . They have a similar luminosity law to Faucher-Giguère & Kaspi (2006) and hence a large number of pulsars with long initial periods. We disagree with their findings that short initial periods cannot reproduce the  $P - \dot{P}$  diagram.

### 5.2 Implications

The idea that a time-variable braking index is a key component in the evolution of pulsars in the  $P - \dot{P}$  diagram leads to some testable predictions. First, as seen in Figure 2, old pulsars move vertically in  $P - \dot{P}$  space and should have large values of  $n$ . For a pulsar with  $P \sim 1$  s,  $\dot{P} \sim 10^{-15.5}$  and  $n \sim 1000$  it may be possible to measure  $\ddot{\nu}$  over a 20 yr period. Intriguingly, in the compilation of Johnston & Galloway (1999), the two pulsars with the largest values of  $P$  also have large values of  $n$ . Secondly, pulsars with smaller values of  $\alpha$  will have larger values of  $n$  and this also applies to young pulsars where  $n$  is more easily measurable. A further interesting test would therefore be to try and measure  $n$  for a group of young pulsars with known  $\alpha$  such as the sample of Rookyard et al. (2015).

In our simulation, all pulsars are born with  $P = 20$  ms. Clearly this is a simplification of the true picture but the observational evidence is strong that initial spin periods are less than 150 ms for a large fraction of the population. In contrast to our results, the best model of Faucher-Giguère & Kaspi (2006) has 84% of their pulsars have spin periods larger than 150 ms and similarly Gullón et al. (2014) have a uniform distribution of initial periods between 0 and 150 ms as their best fit. In both pa-

pers this appears to be a direct result of their luminosity law and it is hard to reconcile this high fraction with the observational evidence from the known young pulsars.

The results also have implications for the lifespan of pulsars and hence the potentially detectable population. In [Faucher-Giguère & Kaspi \(2006\)](#),  $\tau_c$  is equivalent to the true age and many pulsars live well in excess of  $10^8$  yr before crossing the death line. This is not the case in our work; in general  $\tau_c$  is significantly greater than the true age, especially for older pulsars. For example, only 7% of the detected population from the simulation have true ages greater than  $10^7$  yr whereas 35% have  $\tau_c > 10^7$  yr, similar to that of the known population. Figure 5 shows the cumulative distribution of the characteristic and true ages of the pulsars. In addition to the age differences,  $\alpha$  decay reduces the number of pulsars beaming towards Earth. Our modelling therefore suggests that the population of radio-loud pulsars is only  $2 \times 10^5$  and only 10% of these are beaming towards us, a factor of  $\sim 5$  less than the [Faucher-Giguère & Kaspi \(2006\)](#) result but close to the [Lorimer et al. \(2006\)](#) result. This indicates that estimates for how many pulsars the Square Kilometre Array will find ([Keane et al. 2015](#)) may be somewhat overestimated.

## 6 CONCLUSIONS

Nearly fifty years after the discovery of the first radio pulsar, their time-evolution remains a source of debate. Two topics in particular remain a constant thread, the first being the decay (or not) of the magnetic field, the second being their birth parameters. The literature generally favours a lack of field decay except through accretion and relatively large spin periods at birth making the Crab pulsar an exception.

In this paper we show the importance of the decay of the inclination angle between the magnetic and spin axes, an idea which has firm footing in the literature. This decay has two main effects. First it reduces the detectability of older pulsars, as small  $\alpha$  reduces the beaming fraction and increases the observed pulse width. Secondly, it modifies the spin-down evolution so that pulsars no longer follow a track with constant slope in the  $P - \dot{P}$  diagram.

Although we have not attempted a full-blown population analysis, we have shown that it is possible to have all pulsars be born with parameters similar to that of the Crab pulsar and still reproduce the bulk of the features of the known population obviating the need for magnetic field decay or pulsars with long initial spin periods. If these ideas are correct, the birth rate of pulsars is 1 per 100 yr and there are only  $\sim 20000$  pulsars beaming towards Earth.

## ACKNOWLEDGMENTS

We thank M. Kramer and T. Tauris for useful discussions. We used the ATNF pulsar catalogue at <http://www.atnf.csiro.au/people/pulsar/psrcat/> for this work.

## REFERENCES

- Alpar M. A., Cheng A. F., Ruderman M. A., Shaham J., 1982, *Nature*, 300, 728
- Alvarez C., Carramiñana A., 2004, *A&A*, 414, 651
- Antonopoulou D., Weltevrede P., Espinoza C. M., Watts A. L., Johnston S., Shannon R. M., Kerr M., 2015, *MNRAS*, 447, 3924
- Archibald R. F. et al., 2016, *ApJ*, 819, L16
- Archibald R. F., Kaspi V. M., Beardmore A. P., Gehrels N., Kennea J. A., 2015, *ApJ*, 810, 67
- Bates S. D., Lorimer D. R., Rane A., Swiggum J., 2014, *MNRAS*, 439, 2893
- Belczynski K., Lorimer D. R., Ridley J. P., Curran S. J., 2010, *MNRAS*, 407, 1245
- Brook P. R., Karastergiou A., Buchner S., Roberts S. J., Keith M. J., Johnston S., Shannon R. M., 2014, *ApJ*, 780, L31
- Brook P. R., Karastergiou A., Johnston S., Kerr M., Shannon R. M., Roberts S. J., 2016, *MNRAS*, 456, 1374
- Dewey R. J., Taylor J. H., Weisberg J. M., Stokes G. H., 1985, *ApJ*, 294, L25
- Espinoza C. M., Lyne A. G., Kramer M., Manchester R. N., Kaspi V. M., 2011, *ApJ*, 741, L13
- Faucher-Giguère C.-A., Kaspi V. M., 2006, *ApJ*, 643, 332
- Gil J., Gronkowski P., Rudnicki W., 1984, *A&A*, 132, 312
- Goldreich P., Reisenegger A., 1992, *ApJ*, 395, 250
- Gonthier P. L., Ouellette M. S., Berrier J., O'Brien S., Harding A. K., 2002, *ApJ*, 565, 482
- Gonthier P. L., Van Guilder R., Harding A. K., 2004, *ApJ*, 604, 775
- Gullón M., Miralles J. A., Viganò D., Pons J. A., 2014, *MNRAS*, 443, 1891
- Gunn J. E., Ostriker J. P., 1970, *ApJ*, 160, 979
- Hamil O., Stone J. R., Urbanec M., Urbancová G., 2015, *Phys. Rev. D*, 91, 063007
- Igoshev A. P., Popov S. B., 2015, *Astronomische Nachrichten*, 336, 831
- Johnston S., Galloway D., 1999, *MNRAS*, 306, L50
- Jones P. B., 1976, *ApJ*, 209, 602
- Keane E. et al., 2015, *Advancing Astrophysics with the Square Kilometre Array (AASKA14)*, 40
- Keane E. F., Kramer M., 2008, *MNRAS*, 391, 2009
- Kerr M., Hobbs G., Johnston S., Shannon R. M., 2016, *MNRAS*, 455, 1845
- Kramer M., Lyne A. G., O'Brien J. T., Jordan C. A., Lorimer D. R., 2006, *Science*, 312, 549
- Kramer M., Wielebinski R., Jessner A., Gil J. A., Seiradakis J. H., 1994, *A&AS*, 107
- Lorimer D. R., 2004, in *IAU Symposium*, Vol. 218, Camilo F., Gaensler B. M., ed, *Young Neutron Stars and Their Environments*, p. 105
- Lorimer D. R., Bailes M., Harrison P. A., 1997, *MNRAS*, 289, 592
- Lorimer D. R. et al., 2006, *MNRAS*, 372, 777
- Lorimer D. R. et al., 2004, *MNRAS*, 347, L21
- Lyne A., Graham-Smith F., Weltevrede P., Jordan C., Stappers B., Bassa C., Kramer M., 2013, *Science*, 342, 598
- Lyne A., Hobbs G., Kramer M., Stairs I., Stappers B., 2010, *Science*, 329, 408
- Marshall F. E., Guillemot L., Harding A. K., Martin P.,

- Smith D. A., 2016, *ApJ*, 827, L39  
Mitra D., Rankin J. M., 2002, *ApJ*, 577, 322  
Payne D. J. B., Melatos A., 2004, *MNRAS*, 351, 569  
Perera B. B. P., McLaughlin M. A., Cordes J. M., Kerr M.,  
Burnett T. H., Harding A. K., 2013, *ApJ*, 776, 61  
Philippov A., Tchekhovskoy A., Li J. G., 2014, *MNRAS*,  
441, 1879  
Ridley J. P., Lorimer D. R., 2010, *MNRAS*, 404, 1081  
Rookyard S. C., Weltevrede P., Johnston S., 2015, *MNRAS*, 446, 3367  
Shannon R. M. et al., 2013, *ApJ*, 766, 5  
Tauris T. M., Konar S., 2001, *A&A*, 376, 543  
Tauris T. M., Manchester R. N., 1998, *MNRAS*, 298, 625  
Vivekanand M., Narayan R., 1981, *Journal of Astrophysics  
and Astronomy*, 2, 315  
Vranesevic N. et al., 2004, *ApJ*, 617, L139  
Weltevrede P., Johnston S., 2008, *MNRAS*, 387, 1755

This paper has been typeset from a  $\text{\LaTeX}$  file prepared  
by the author.